blood®
Regular Article

THROMBOSIS AND HEMOSTASIS

Microlyse: a thrombolytic agent that targets VWF for clearance of microvascular thrombosis

Steven de Maat,[1] Chantal C. Clark,[1] Arjan D. Barendrecht,[1] Simone Smits,[1] Nadine D. van Kleef,[1] Hinde El Otmani,[1] Manon Waning,[1] Marc van Moorsel,[1] Michael Szardenings,[2,3] Nicolas Delaroque,[3] Kristof Vercruysse,[4] Rolf T. Urbanus,[1] Silvie Sebastian,[1] Peter J. Lenting,[5] Christoph Hagemeyer,[6] Thomas Renné,[7] Karen Vanhoorelbeke,[8] Claudia Tersteeg,[8] and Coen Maas[1]

[1]Central Diagnostic Laboratory Research, University Medical Center Utrecht, Utrecht University, Utrecht, The Netherlands; [2]Epitopic, Leipzig, Germany; [3]Ligand Development Unit, Fraunhofer IZI, Leipzig, Germany; [4]TargED Biopharmaceuticals, Utrecht, The Netherlands; [5]Laboratory for Haemostasis, Inflammation and Thrombosis, INSERM Unité Mixte de Recherche 1176, Université Paris-Saclay, Le Kremlin-Bicêtre, France; [6]Australian Centre for Blood Diseases, Monash University, Melbourne, Australia; [7]Institute for Clinical Chemistry and Laboratory Medicine, University Medical Center Hamburg-Eppendorf, Hamburg, Germany; and [8]Laboratory for Thrombosis Research, KU Leuven Campus Kulak Kortrijk, Kortrijk, Belgium

KEY POINTS

- **We developed a thrombolytic fusion protein that targets VWF for plasmin-dependent degradation of fibrin-poor microthrombi.**
- **This strategy is superior to blockade of platelet-VWF interactions in a preclinical mouse model for microvascular thrombosis.**

Thrombotic microangiopathies are hallmarked by attacks of disseminated microvascular thrombosis. In thrombotic thrombocytopenic purpura (TTP), this is caused by a rise in thrombogenic ultra-large von Willebrand factor (VWF) multimers because of ADAMTS13 deficiency. We previously reported that systemic plasminogen activation is therapeutic in a TTP mouse model. In contrast to its natural activators (ie, tissue plasminogen activator and urokinase plasminogen activator [uPA]), plasminogen can directly bind to VWF. For optimal efficacy and safety, we aimed to focus and accelerate plasminogen activation at sites of microvascular occlusion. We here describe the development and characterization of Microlyse, a fusion protein consisting of a high-affinity V_HH targeting the CT/CK domain of VWF and the protease domain of uPA, for localized plasminogen activation on microthrombi. Microlyse triggers targeted destruction of platelet-VWF complexes by plasmin on activated endothelial cells and in agglutination studies. At equal molar concentrations, Microlyse degrades microthrombi sevenfold more rapidly than blockade of platelet-VWF interactions with a bivalent humanized V_HH (caplacizumab*). Finally, Microlyse attenuates thrombocytopenia and tissue damage (reflected by increased plasma lactate dehydrogenase activity, as well as PAI-1 and fibrinogen levels) more efficiently than caplacizumab* in an ADAMTS13$^{-/-}$ mouse model of TTP, without affecting hemostasis in a tail-clip bleeding model. These findings show that targeted thrombolysis of VWF by Microlyse is an effective strategy for the treatment of TTP and might hold value for other forms of VWF-driven thrombotic disease.

Introduction

Thrombotic microangiopathies are a collection of disorders in which catastrophic disseminated thrombosis of the microvasculature is a central feature.[1] In thrombotic thrombocytopenic purpura (TTP), this is caused by ADAMTS13 deficiency. This is generally the result of autoantibodies against ADAMTS13, which clear and neutralize the protease (acquired TTP [aTTP]). TTP has an unpredictable episodic nature, and acute attacks are hallmarked by deep consumptive thrombocytopenia: microthrombi that occlude the vasculature, deplete the systemic circulation from platelets. This leads to ischemic injury in various tissues, accompanied by a severe risk of bleeding. The current standard of care for acute aTTP attacks includes plasma exchange to remove autoantibodies and restore ADAMTS13 activity. Long-term therapeutic strategies include immune modulation to reduce autoantibody levels.

The interaction between platelet glycoprotein Ibα (GPIbα) and von Willebrand Factor (VWF) drives the formation of microthrombi in TTP. This does not require platelet activation, coagulation system activation, or fibrin formation.[2] Recently, a bivalent single-chain antibody (V_HH; nanobody) that blocks the binding of platelets to the VWF A1 domain for treatment of aTTP was developed. Administration of this nanobody (INN: caplacizumab) in combination with plasma exchange shortens acute TTP attack duration from 5 days to 3 to 4 days. This was demonstrated by a faster normalization of the platelet count[3] and reduced need for plasma exchange (by 39%), which has a large impact on the organ damage that patients sustain during attacks.[4] In essence, shortening the attack duration is critical to the management of TTP.

We previously found evidence for activation of endogenous plasminogen in patients during TTP attacks.[5,6] We proposed an

auxiliary role of plasmin as a VWF-cleaving enzyme in this setting and subsequently demonstrated that systemic plasminogen activation (with a bacterial plasminogen activator) attenuated thrombocytopenia in a murine TTP model.[5] Subsequently, we demonstrated that endogenous plasminogen activation regulates disease severity in a mouse model for aTTP.[6] These findings led us to believe that exploiting the VWF-cleaving properties of plasmin holds therapeutic value. While plasminogen can directly bind to VWF in a lysine-dependent manner,[5] neither tissue plasminogen activator (tPA) nor urokinase plasminogen activator (uPA) can bind VWF directly. Strategies to bring plasminogen activators to VWF should hold value for the treatment of TTP.

We here set out to develop a new thrombolytic agent for the destruction of platelet-VWF complexes. Two forms of platelet-targeting thrombolytic agents are currently under development. Firstly, an innovative sc-Fv against glycoprotein IIb/IIIa (GPIIb/IIIa) was fused to the protease domain of uPA.[7] This fusion protein only binds to this platelet-specific integrin in its activated state, which requires platelet activation. A similar compound against GPIIb/IIIa was developed that does not require platelet activation but does require thrombin for zymogen activation.[8] However, TTP is considered a fibrin-poor thrombotic disorder,[2] and the critical interaction between GPIbα and VWF does not require platelet activation.[9] We, therefore, engineered a VWF-targeting plasminogen activator for plasmin-mediated destruction of platelet-VWF complexes that is not critically dependent on the presence of fibrin-, thrombin-, or platelet activation.

Methods

A detailed list of reagents and methods is supplied in the supplemental Data.

Disruption of VWF-platelet agglutinates in vitro

Blood platelets were isolated from citrated human whole blood as previously described.[5] Platelets (200.000/μL) were incubated with VWF (5 μg/mL), plasminogen (100 μg/mL), and the platelet aggregation inhibitors RGDW (200 μM) and iloprost (0.4 μg/mL) for 15 minutes at 37°C in a light transmission aggregometer while mixing at 900 rpm. Platelet agglutination was triggered with ristocetin (0.6 mg/mL). After 6 minutes, the Microlyse variants (1 μg/mL; 20.7 nM) or caplacizumab* (0.67 μg/mL; 20.7 nM) were added and agglutinate lysis was monitored. For all samples, time points were determined at which microthrombi were lysed by 50% (ie, from the moment of adding the constructs). Results were processed in GraphPad Prism 9.2 and analyzed by 1-way ANOVA.

After these experiments, samples were fixed immediately in 2 mL formaldehyde in HT buffer (0.15% wt/vol in HEPES-Tyrode; 10 mM HEPES, 145 mM NaCl, 5 mM KCl, 0.5 mM Na_2HPO_4, 1 mM $MgSO_4$, pH = 7.4) for 10 minutes and centrifuged 15 minutes at 500 × g. Pellets were resuspended in 150 μL rabbit anti-urokinase polyclonal antibody (1 μg/mL in HEPES Tyrode's [HT] buffer, pH = 7.4) for 45 minutes at room temperature (RT). After adding 1 mL of formaldehyde in HT buffer, the samples were centrifuged for 15 minutes at 500 × g, and the pellet was resuspended in 150 μL goat anti-rabbit-Alexa488 (1 μg/mL in HT pH = 7.4). After 45 minutes at RT, 2 mL of formaldehyde in HT buffer was added, and samples were analyzed by FACS (Canto II).

In vivo efficacy and safety of Microlyse and caplacizumab* in a TTP mouse model

All animal studies were performed at the animal institution of KU Leuven in accordance with protocols approved by the Institutional Animal Care and Use Committee (project numbers: P009/2020, P051/2021). Female and male *Adamts13*$^{-/-}$ mice (CASA/Rk-C57BL/6J-129X1/SvJ background) of 8 to 12 weeks old were used. Blood was collected at baseline (7 days prior to TTP challenge) in either trisodium citrate (5:1 vol/vol of blood: 3% trisodium citrate) or EDTA (10:1 vol/vol of blood: 0.5 M EDTA). To induce TTP, mice were anesthetized using isoflurane and intravenously injected with 2250 U/kg recombinant human VWF (rhVWF; Takeda, Vienna, Austria). After 15 minutes, mice were given an IV injection with saline, Microlyse variants, or caplacizumab*. Throughout our studies, we assumed a circulating blood volume in mice of 80 mL/kg.

Tail-clip bleeding model Thirty minutes after TTP induction (ie, 15 minutes after treatment initiation), hemostasis was evaluated using the tail-clip bleeding assay. Hereto, a segment of 5 mm was amputated from the distal end of the tail, using a scalpel, and the tail was immediately immersed in 0.9% NaCl at 37°C. The time until the blood loss ceased completely was monitored up to 600 seconds. Finally, blood was collected in EDTA via retro-orbital puncture, where after the mice were sacrificed by cervical dislocation. Total blood cell counts were analyzed on EDTA blood samples within 30 minutes after blood draw, with a Hemavet 950 hematology system (Drew Scientific, Dallas, TX).

Mice that did not undergo the tail-clip procedure were terminated 24 hours after TTP induction, and whole blood was collected for further analysis. Plasma was isolated from citrated blood samples by centrifugation at 2000 × g for 10 minutes and stored at -80°C. Total blood cell counts were analyzed in EDTA blood samples within 30 minutes after blood draw with a Hemavet 950 hematology system. Mice were sacrificed under deep anesthesia with isoflurane. Blood smears were made from EDTA blood, stained with May-Grünwald-Giemsa, and analyzed using a light microscope (Zeiss).

Lactate dehydrogenase (LDH) activity LDH activity was measured in citrated plasma samples using an LDH activity colorimetric assay kit (Biovision, Milpitas, CA) according to the manufacturer's instructions.

Results

Development and biochemical characterization of Microlyse

ADAMTS13 cleaves VWF in its A2 domain while plasmin cleaves in the linker sequence between the A1 and A2 domains (schematic overview in supplemental Figure 1A); both cleavage events require VWF unfolding and lower its thrombogenicity.[10,11] Plasminogen binds to VWF and the recombinant VWF A1 domain in a lysine-dependent manner.[5] We fused anti-VWF V_HH's to the protease domain of human uPA (mini-uPA) via a Gly/Ser-linker, to develop a VWF-targeting plasminogen activator for localized plasminogen activation (called Microlyse)

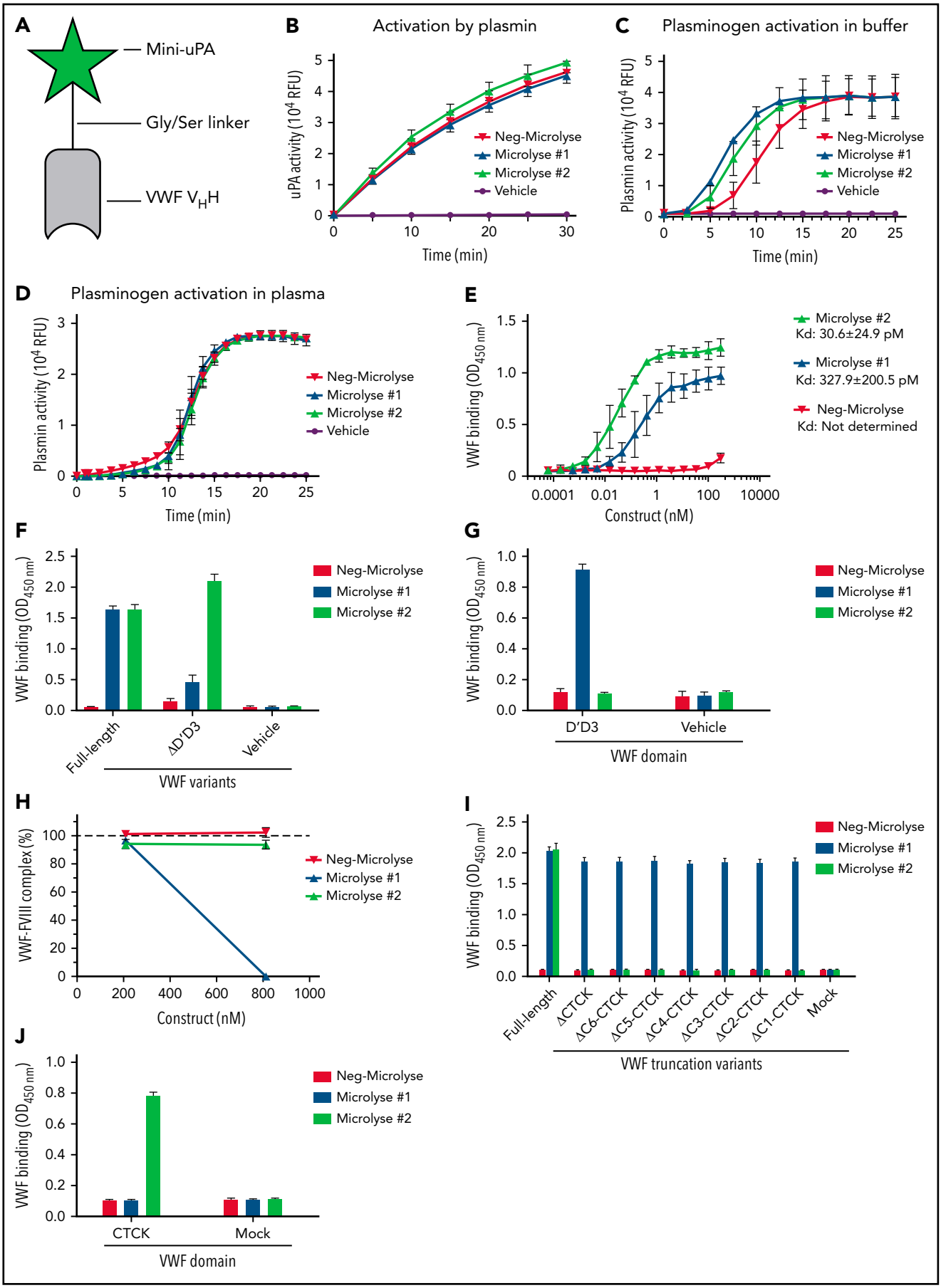

Figure 1. Microlyse design and characteristics. (A) Microlyse design. Microlyse is a single polypeptide composed of the enzymatic domain of uPA, fused together with a VWF-targeting V_HH through a glycine-serine linker sequence. (B) Microlyse variants (20.7 nM) gain urokinase-like activity in buffer after activation by 11.6 nM

(Figure 1A). Hereto, we selected 2 distinct anti-VWF V_HH's as targeting moieties (resulting in Microlyse variants #1 and #2). We developed a third Microlyse variant (Neg-Microlyse) containing a nontargeting V_HH as a negative control. The V_HH (R2) in Neg-Microlyse was raised against the exogenous azo-dye Reactive Red 6 and is commonly used as a negative control in various animal studies.[12,13] We chose the catalytic domain of uPA as a plasminogen activator due to its characteristic intrinsic single-chain activity,[14] which efficiently drives autocatalytic, reciprocal plasminogen activation.[15]

All 3 Microlyse variants express as single-chain molecules (supplemental Figure 1B) and do not display detectable enzymatic activity after purification (supplemental Figure 1C). They develop enzymatic activity after activation by plasmin (Figure 1B) and support autocatalytic plasminogen activation in a buffered system, as well as in plasma (Figure 1C and D, respectively). These experiments show that these Microlyse variants are produced in a zymogen state that can initiate plasminogen activation, similar to full-length uPA.

Binding studies show that both Microlyse variants bind with high apparent affinities to immobilized VWF (Figure 1E), whereas Neg-Microlyse does not. Moreover, all Microlyse variants are incapable of binding to immobilized fibrin (supplemental Figure 1D). In contrast, tPA selectively binds to fibrin, but not to VWF (supplemental Figure 1D and E, respectively).

VWF supports several critical interactions: factor VIII (FVIII) binding is mediated through sequences within the D'D3 of VWF,[16] while collagen- and platelet binding is mediated through its A-domains. Finally, the VWF D4-C1 domains support binding to platelet glycoprotein IIb/IIIa and ADAMTS13. To rule out potential adverse effects, we set out to determine the exact binding epitope for the Microlyse variants on VWF.

Microlyse #1 and #2, but not Neg-Microlyse, capture recombinant full-length VWF from solution (Figure 1F). Similarly, both Microlyse #1 and #2 capture VWF from plasma of multiple species, although Microlyse #2 reacted with a broader range of species than Microlyse #1 (supplemental Figure 1G). None of the Microlyse variant captures recombinant A1-A3 domains, while the bivalent single-domain antibody caplacizumab* (caplacizumab, but with an N-terminal His6-tag and C-terminal Myc-tag) captures it successfully (supplemental Figure 1H). This is in line with its binding site in the VWF A1 domain.[17] In contrast, both Microlyse #1 and #2, as well as caplacizumab*, captured a VWF deletion mutant lacking the D4-C1 domains (supplemental Figure 1I). Together these findings rule out the centrally positioned A1-C1 domains as binding sites for both Microlyse variants (VWF schematic overview) (supplemental Figure 1A), leaving the N-terminal D'D3 domains and C-terminal C2-CT/CK domains for further investigation.

We next identified that Microlyse #1 is unable to capture a VWF-truncation variant lacking the N-terminal D'D3 assembly, while Microlyse #2 does (Figure 1F). Conversely, Microlyse #1 is able to capture recombinant VWF D'D3 domains, while Microlyse #2 cannot (Figure 1G). Interestingly, Microlyse #1 disrupts the binding of FVIII to VWF in plasma, while Microlyse #2 does not (Figure 1H). Together these experiments show that Microlyse #1 binds to the D'D3 assembly and competes with FVIII.

As it does not bind to any of the domains between D'D3 and C1, Microlyse #2 should bind to the C-terminal C2-CT/CK region of VWF. We next developed C-terminal VWF truncation variants (expression data in supplemental Figure 1J) to further identify the correct domain. Microlyse #2 captures full-length VWF, but not any of the variants lacking the CT/CK domain (Figure 1I), whereas Microlyse #1 does. Conversely, only Microlyse #2 captures recombinant CT/CK domain (Figure 1J; expression data in supplemental Figure 1K). These data demonstrate that the binding site for Microlyse #2 is located within the CT/CK domain.

Finally, confocal microscopy confirms that Microlyse (without plasminogen) binds to elongated platelet/VWF complexes that form on the surface of activated HUVEC ("beads on a string"). Indeed, both Microlyse variants and caplacizumab*, but not Neg-Microlyse or tPA, bind to these strings (Figure 2A; compounds in green, platelets in red). In flow cytometry experiments, we triggered VWF binding to platelets in diluted whole blood with ristocetin. Under these conditions, Microlyse is recruited to platelets in a VWF-dependent manner, while Neg-Microlyse is not (Figure 2B). As disruption of FVIII binding is undesirable to the safety profile of Microlyse, and Microlyse #2 has better binding properties, we selected Microlyse #2 as our lead compound for further investigation, naming it Microlyse from here on forward.

Functional properties of Microlyse

Microlyse was designed to bind to VWF, which should act as a template for plasminogen activation. In a series of experiments, plasmin generation by Microlyse was examined with a fluorogenic substrate in the presence of globular VWF or open VWF (VWF and ristocetin). Here, open VWF accelerated plasmin generation in the presence of Microlyse, and, to a lesser extent, by Neg-Microlyse (Figure 3A-B; note that ristocetin does not exclusively bind VWF[18]). By comparison, the targeting properties of Microlyse in these experiments under static conditions accelerate plasminogen activation ~2-fold, and the maximal plasmin activity in assay is ~20% higher (Figure 3C and D, respectively). In short, open VWF polymers form a template for Microlyse-dependent plasminogen activation.

In a similar manner, we explored the thrombolytic properties of platelet-VWF complexes in a buffered system. Platelet agglutination was triggered in cuvettes by adding ristocetin to washed platelets in the presence of VWF and plasminogen (where indicated) while stirring. Microlyse or controls were added 6 minutes after initiation of agglutination. Under these near-static conditions, microthrombi first form and can subsequently be degraded

Figure 1 (continued) plasmin. (C) Microlyse variants (20.7 nM) activate 1.16 μM plasminogen in buffer. (D) Microlyse variants (207 nM) activate plasminogen in plasma. (E) Binding of Microlyse variants to immobilized VWF. (F) Capture of full-length VWF or a VWF variant lacking the D'D3 domain (ΔD'D3) by immobilized Microlyse variants. (G) Capture of recombinant D'D3 by immobilized Microlyse variants. (H) VWF-FVIII complexes in plasma after incubation with Microlyse variants. (I,J) Capture of full-length VWF, C-terminal VWF truncation variants, or recombinant CT/CK domain by immobilized Microlyse variants. Data represent the mean ± SD of 3 separate experiments, each performed in duplicate.

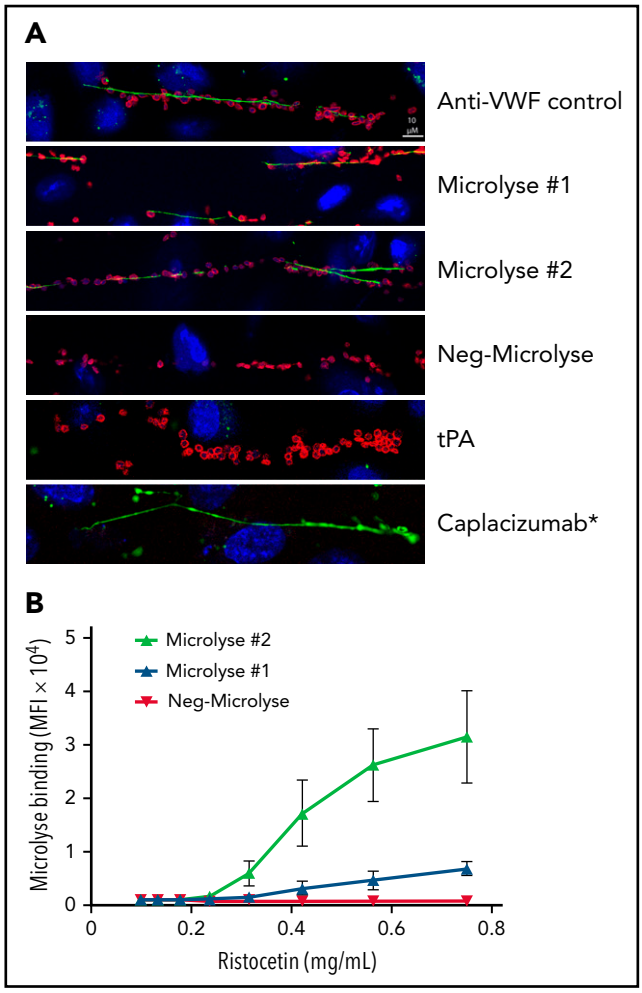

Figure 2. Microlyse binds to VWF on the surface of cultured endothelial cells under flow. (A) Binding of Microlyse #1 and #2 (62.1 nM) to VWF on histamine-stimulated endothelial cells under flow. Endothelial cells were stained after fixation with DAPI (blue), and platelets were stained with anti-GPIbα-APC (red). VWF and Microlyse variants were stained with specific antibodies (green). tPA or caplacizumab* were coupled to Alexa488 (green). Images are representative of 3 separate experiments. (B) Binding of Microlyse variants to platelets in ristocetin-treated whole blood, determined by flow cytometry. Data represent the mean ± SD of 3 separate experiments, each performed in duplicate.

(Figure 3E). It takes approximately 2 minutes after addition of Microlyse to achieve 50% degradation in a plasminogen-dependent manner (Figure 3F). By comparison, nontargeting Neg-Microlyse degrades microthrombi by 50% in approximately 8 minutes, due to plasminogen activation in solution (Figure 1C; PAI-1 and α2-antiplasmin are absent in buffered systems) (Figure 3E-F). The difference in degradation rates between Microlyse and Neg-Microlyse show the advantage of targeted delivery of mini-uPA for degradation of microthrombi in this near-static system. After degradation, Microlyse remains associated with approximately 30% of platelets in solution (supplemental Figure 2A), suggesting that it is retained via a cleavage fragment of VWF. We confirmed that Microlyse binds to immobilized VWF after complete plasmin cleavage in vitro (supplemental Figure 2B-C).

Caplacizumab has recently been authorized for the treatment of aTTP, and clinical experience with this therapy is growing.[19] Caplacizumab* disrupts preformed microthrombi at a much slower rate than Microlyse. It takes caplacizumab* approximately 29 minutes to dissolve microthrombi by 50% (Figure 3G-H) at an equal molar concentration as was used for Microlyse (Figure 3E-F).

In the next series of experiments, we compared the efficacy of Microlyse to caplacizumab* in their ability to disrupt platelet-VWF complexes under flow in ADAMTS13-inactivated plasma on histamine-stimulated HUVEC. In a control setting (vehicle), there is gradual accumulation of platelet-VWF complexes on the endothelial cell surface (Figure 4A; platelets are highlighted in red). Figure 4B and supplemental Figure 3A show quantification of the number and total length of platelet-VWF complexes on the HUVEC surface. The addition of Microlyse to the flow system, 8 minutes after initiating platelet-VWF complex formation, prevents further accumulation and removes platelet-VWF complexes from the HUVEC surface in a targeted manner (Figure 4A-D,G; supplemental Figure 3A-C,F).

In this model, an equal concentration of caplacizumab* (but not tPA) disrupts platelet-VWF complexes with comparable efficiency to Microlyse (Figure 4A,E-G; supplemental Figure 3D-F). In control experiments, we confirmed that activated Microlyse is inhibited by PAI-1 with similar efficiency as activated (2-chain) uPA (supplemental Figure 3G-H). Furthermore, the antifibrinolytic agent tranexamic acid (TXA) fully protects platelet-VWF complexes from plasmin-mediated degradation. Finally, reconstitution of ADAMTS13-inactivated plasma with recombinant ADAMTS13 destroys these complexes (supplemental Figure 3I).

Microlyse attenuates thrombotic microangiopathy in vivo

In earlier studies, we demonstrated that systemic plasminogen activation attenuates key features of TTP in *Adamts13*-deficient mice.[5] Here, we explored the therapeutic value of Microlyse in this model (outlined in Figure 5A). Murine versions of Microlyse and Neg-Microlyse were prepared by replacing the human mini-UPA domain for the murine version. We triggered TTP attacks in *Adamts13*-deficient mice by IV administration of an overdose of human recombinant VWF (2250 IU/kg). Fifteen minutes later, mice were treated with either Microlyse, Neg-Microlyse, caplacizumab*, or saline (vehicle). After 24 hours, saline-treated mice showed profound thrombocytopenia, which is characteristic of the consumptive microthrombosis of TTP (Figure 5B). Furthermore, plasma lactate dehydrogenase (LDH) activity and PAI-1 levels were increased as a result of the ongoing microangiopathy and endothelial injury (Figure 5C and D, respectively).[20]

Treatment with Microlyse dose-dependently attenuates thrombocytopenia (Figure 5B; confirmed by blood smears in supplemental Figure 4) and fully corrects LDH activity and PAI-1 levels back to baseline (Figure 5C and D, respectively). In contrast, administration of Neg-Microlyse does not attenuate thrombocytopenia, nor does it correct elevated LDH activity or PAI-1 levels. Together, these findings demonstrate the value of targeting thrombolytic activity to VWF in vivo.

The reported maximal concentration of caplacizumab in plasma of human subjects is 63.26 nM (1765 ng/mL; IV administration[3]) or 21.51 nM (600 ng/mL; subcutaneous administration[21]). In our

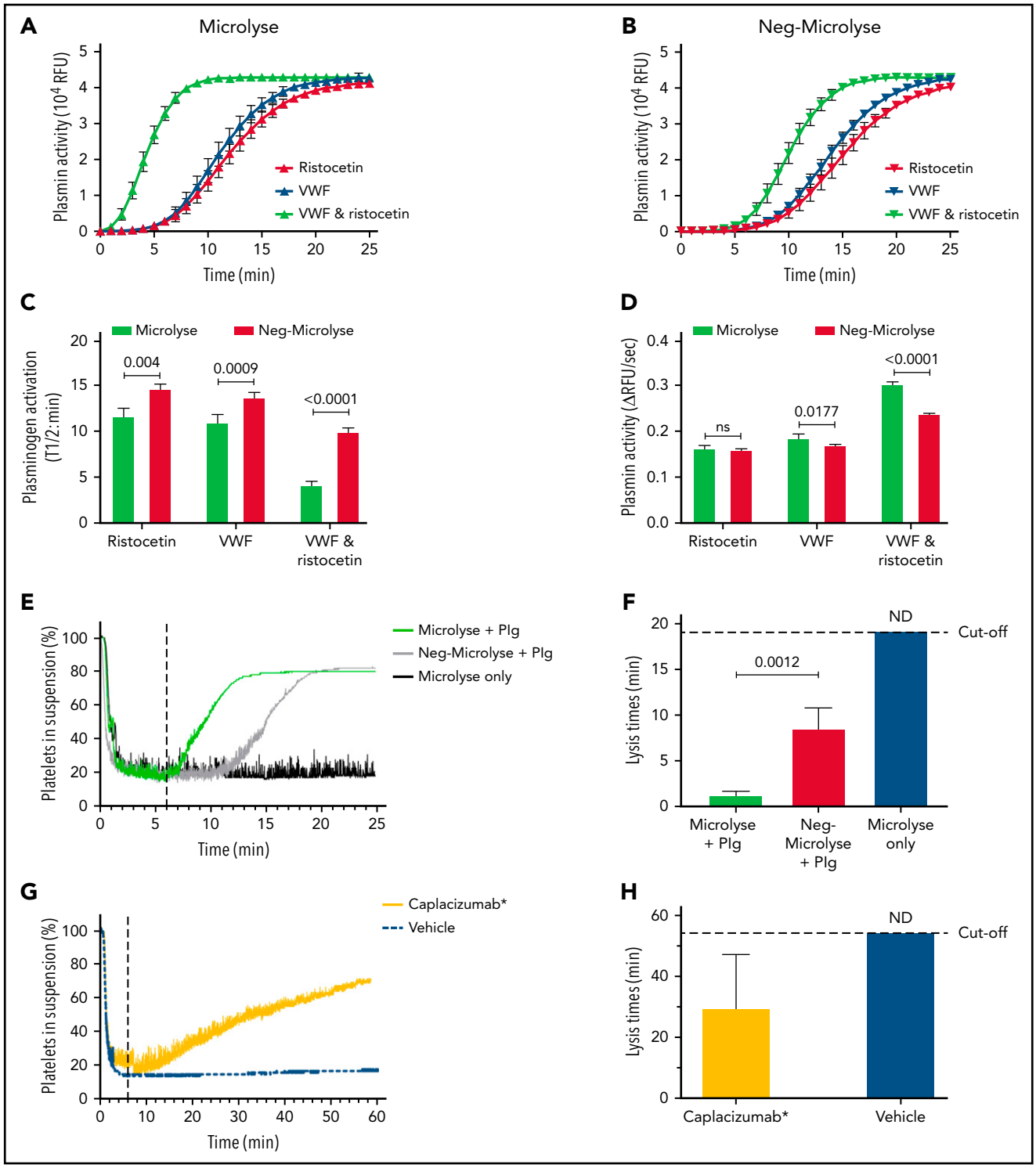

Figure 3. Microlyse degrades platelet-VWF complexes. (A) Plasminogen activation by Microlyse in the presence of globular VWF (VWF), open VWF (VWF & ristocetin), or vehicle (ristocetin). (B) Plasminogen activation by Neg-Microlyse in the presence of globular VWF (VWF), open vWF (VWF & ristocetin), or vehicle (ristocetin). (C). Time to half maximal plasmin activity (in minutes). (D) Maximal rates of fluorogenic substrate conversion (ΔRFU/sec). (C,D) Data represent the mean ± SD of 3 separate experiments. Comparisons were made by 2-way ANOVA with Bonferroni's multiple comparison test. (E) Lysis of ristocetin-induced platelet agglutinates by Microlyse variants (20.7 nM; added at t = 6 minutes, indicated by dotted lines) in absence or presence of (1.16 μM) plasminogen. Data are representative of 3 separate experiments. (F) Lysis times (ie, time to reach 50% agglutinate lysis after addition of compounds). Data represent the mean ± SD of 3 separate experiments. Comparisons were made to Neg-Microlyse by 1-way ANOVA with post hoc Dunnett's multiple comparison test. (G) Disruption of ristocetin-induced platelet agglutination by caplacizumab* (20.7 nM; added at t = 6 minutes, indicated by dotted lines). (H) Lysis times (ie, time to reach 50% agglutinate lysis after addition of caplacizumab*). Data represent the mean ± SD of 3 separate experiments. Comparisons were made by unpaired Student *t* test with Welch's correction.

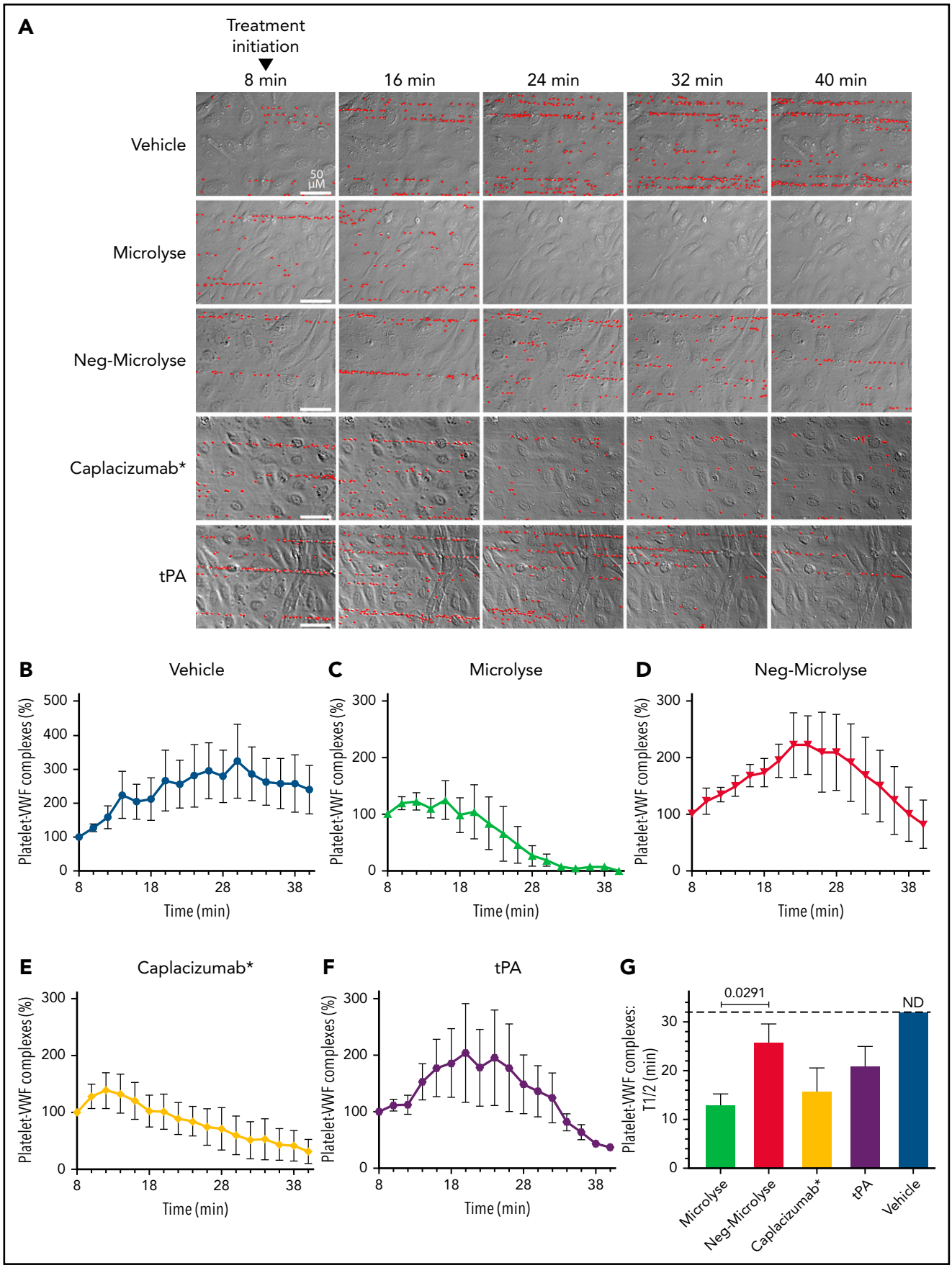

Figure 4. Microlyse degrades platelet-VWF strings on endothelial cells in ADAMTS13-inactivated plasma. (A) Time-lapse morphology of platelet-covered VWF strings on histamine-stimulated endothelial cells in ADAMTS13-inactivated plasma, after addition of Microlyse variants, caplacizumab*, or tPA (207 nM each). Bound platelets are highlighted in red. (B-F) Time-dependent lysis of platelet-VWF complexes. (G) Time to reach 50% breakdown of platelet-VWF complexes (ie, from treatment initiation). Data represent the mean ± SEM of 4 separate experiments. Comparisons were made by 1-way ANOVA with post hoc Dunnett's multiple comparison test.

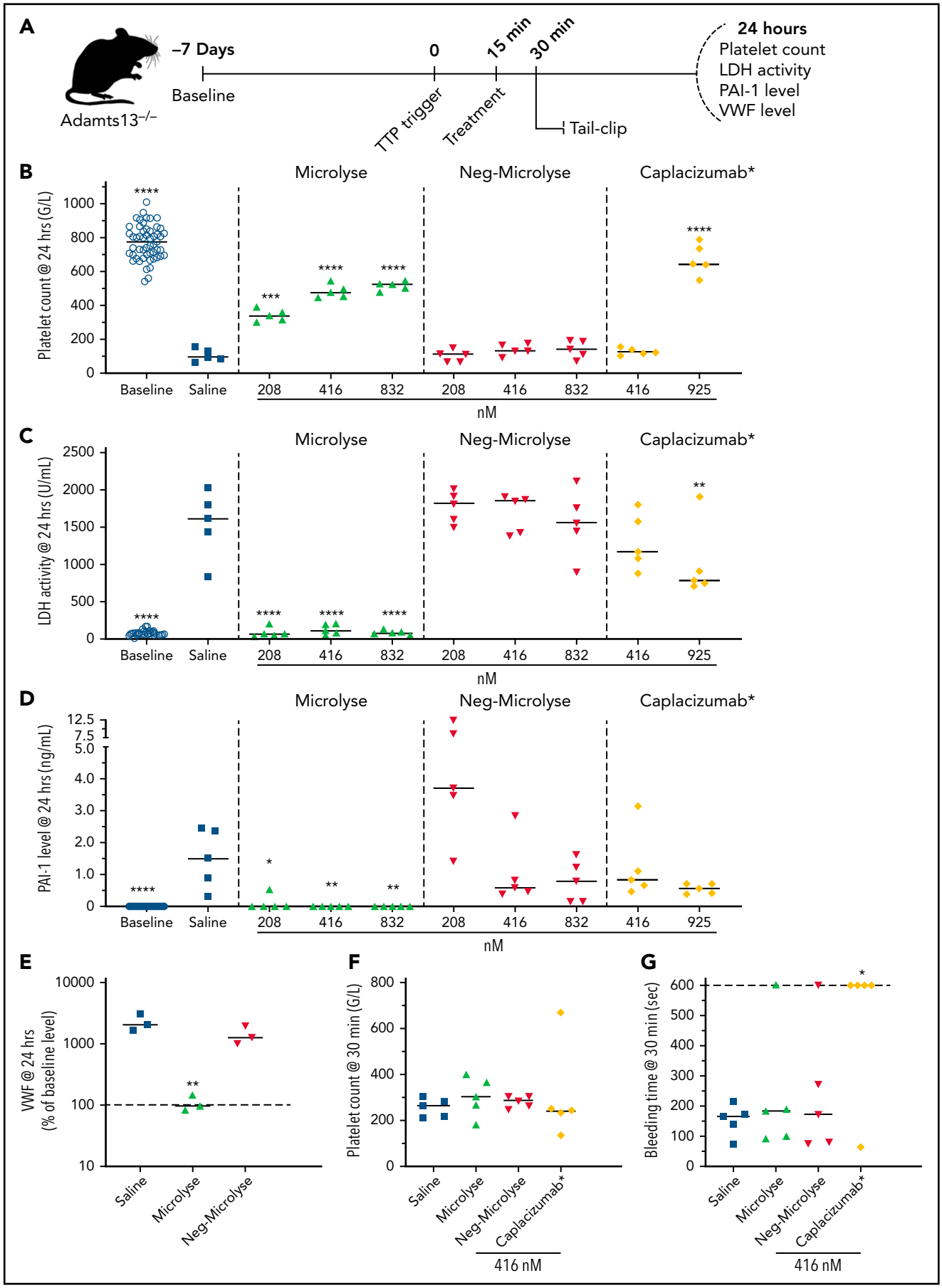

Figure 5. Microlyse attenuates the symptoms of acute TTP in *Adamts13*$^{-/-}$ mice. (A) Experimental setup; 7 days prior to TTP challenge, baseline characteristics (platelet counts, LDH activity, and PAI-1 levels were determined). Mice were challenged with rhVWF (2250 IU/kg). After 15 minutes, mice were IV injected with saline or

TTP model, caplacizumab* (416 nM) does not correct thrombocytopenia while LDH activity and PAI-1 levels remain elevated (Figure 5C-D). At an even higher dose (925 nM), hemocytometric analysis reports increased platelet counts, while blood smears are still devoid of platelets (supplemental Figure 4). Furthermore, LDH activity and PAI-1 levels remain elevated upon treatment with caplacizumab* (Figure 5C and D, respectively). Interestingly, prophylactic administration of caplacizumab* (416 nM; administered before TTP induction) results in partial attenuation of thrombocytopenia, LDH activity, and PAI-1 levels (supplemental Figure 5). This indicates that caplacizumab* is unable to break the ongoing cycle of thrombotic microangiopathy within 24 hours but prevents the build-up of new microthrombi. These insights correspond well to clinical studies and expert recommendations to administer caplacizumab as early as possible.[3,4,19]

The observed correction of thrombocytopenia by Microlyse (Figure 5B) corresponded well to normalization of VWF antigen levels 24 hours after the TTP challenge (Figure 5E). We observed no significant changes in VWF multimer distribution between treatments (supplemental Figure 6A). Interestingly, despite congenital ADAMTS13 deficiency, a shift in multimer size was observed compared with the input material (rhVWF). This was seen earlier in a rat model for TTP, where saline treatment led to time-dependent lowering of multimer size.[22]

Intense thrombolytic treatment may be accompanied by systemic fibrinogenolysis or consumptive plasminogen activation, which translates into an increased risk of bleeding. Western blot analyses showed that fibrinogen levels are increased 24 hours after attack induction in both saline- and Neg-Microlyse-treated mice compared with baseline (supplemental Figure 6B-C). Treatment with Microlyse fully attenuates this (ie, fibrinogen levels are normal), without evidence present for systemic plasminogen consumption (supplemental Figure 6D-E). This suggests that the increased fibrinogen levels during experimental TTP are the result of hepatic tissue injury. This acute-phase reaction can be avoided by Microlyse treatment.

Finally, we investigated possible global hemostatic defects caused by Microlyse in a tail-clip bleeding model, which is sensitive to therapeutic hyperfibrinolysis after tPA or uPA administration.[7,23] TTP attacks were triggered in ADAMTS13-deficient mice, and treatment was administered as before. Fifteen minutes later, the tail injury challenge was executed (outlined in Figure 5A). Platelet counts were equally lowered between groups (Figure 5F) and tail bleeding times were comparable between saline- and Neg-Microlyse- or Microlyse-treated mice (Figure 5G). In comparison, caplacizumab*-treated mice displayed prolonged bleeding times, which matches earlier findings in baboons treated with caplacizumab.[24] Together, these data indicate that targeted thrombolysis is superior in safety compared with blockade of primary hemostasis.

Discussion

We here describe the development of Microlyse, a VWF-targeting thrombolytic agent for the treatment of TTP attacks. The ultimate goal of any treatment of this condition is to reduce the attack duration and limit ischemic tissue damage. We demonstrate that Microlyse acts as a plasminogen activator that binds with high affinity to VWF CT/CK domain (Figure 1). We found that VWF acts as a scaffold for plasminogen activation by Microlyse in a conformation-dependent manner (Figure 3A-D). When bound to VWF polymers on endothelial cells, Microlyse triggers their degradation by plasmin (Figure 4). This mechanism is unlike that of caplacizumab*, which displaces platelets from VWF polymers and inhibits microthrombus build-up. As a result, both agents can disrupt elongated platelet-VWF complexes with comparable efficacy (Figure 4). In contrast, enzymatic degradation of ristocetin-triggered microthrombi by Microlyse is far more efficient than the passive disruption by caplacizumab* at equal molar concentrations (Figure 3E-H).

Similarly, we found that Microlyse attenuates thrombocytopenia in a preclinical in vivo TTP model (Figure 5). This treatment is accompanied by complete normalization of plasma LDH activity, PAI-1 and fibrinogen levels. This indicates that microvascular obstructions have been removed and that ischemic tissue injury has been terminated. By comparison, caplacizumab* is unable to attenuate tissue injury, even when given therapeutically (ie, after disease onset) at exceedingly high doses. This is unlike findings in nonhuman primate studies where caplacizumab showed therapeutic value, but particularly when given before experimental challenge.[24] This suggests that the symptoms of triggered thrombotic microangiopathy in our *Adamts13*-deficient mouse model are more severe than those that spontaneously occur in baboons after administration of an ADAMTS13-inhibiting monoclonal antibody.

The mouse model that was used here was first described in a study on the efficacy of recombinant human ADAMTS13 (rhADAMTS13). The authors described that the administration of 320 U/kg rhADAMTS13 was therapeutic under conditions similar to the ones in the present study.[25] At higher doses, rhADAMTS13 was effective in a rat model for aTTP.[22] By comparison, a currently active (not recruiting) clinical trial is aiming to study the efficacy of administration of 40 ± 4 IU/kg rADAMTS13, twice daily in combination with plasma exchange (https://clinicaltrials.gov/ct2/show/NCT03922308). This dosing is identical to that of the ongoing trial in congenital TTP (https://clinicaltrials.gov/ct2/show/NCT03393975).

The behavior of Neg-Microlyse in our study shows the critical dependence of this strategy on its targeting capacity. Without a VWF-targeting moiety, Microlyse is unable to correct features of TTP in a mouse model, which corresponds to its functional characterization in in vitro experiments. This control protein also shows that plasmin-mediated destruction in vivo is not dependent on systemic plasminogen activation, even at the highest

Figure 5 (continued) treatment compounds. Experimental outcomes were determined either 15 minutes after treatment (t = 30 min; tail-clip) or 24 hours after TTP induction. (B) Platelet counts. (C) LDH activity. (D) PAI-1 levels. (E) VWF antigen levels 24 hours after administration of saline, Microlyse, or Neg-Microlyse (416 nM). (F,G) Platelet counts and bleeding times 15 minutes after administration of saline, Microlyse, or Neg-Microlyse (416 nM). Data are represented as scatterplots with medians. *$P < .05$, **$P < .005$, ***$P < .0005$, ****$P < .0001$, compared with saline by 1-way ANOVA with post hoc Dunnett's multiple comparison test.

concentrations tested (supplemental Figure 6D-E). The repeated observation that plasmin activity corrects thrombocytopenia (the main driver of bleeding in TTP) while eliminating microthrombotic obstructions suggests that our strategy is safer than it might intuitively sound. We hypothesize that, similar to the application of tPA in stroke, the function of Microlyse is controlled by endogenous inhibitors of the plasminogen activation system. Future studies will have to address how and when to apply this agent for optimal efficacy and safety.

Finally, we hypothesize that a VWF-targeting thrombolytic agent may hold value in indications beyond TTP. The application of tPA in conditions like stroke and myocardial infarction has provided a tremendous improvement to the clinical outcomes of these conditions. Nevertheless, tPA is mainly effective in the early phase of stroke development, but later on, the risk of bleeding outweighs its clinical benefit. Despite effective initial recanalization, a large subset of patients experience a perfusion defect as a result of an ischemia-reperfusion injury. Similar observations are made with percutaneous intervention for the treatment of myocardial infarction. It has been demonstrated that administration of recombinant ADAMTS13 to proteolyse VWF polymers improves the outcome in preclinical models for stroke and myocardial ischemia-reperfusion injury.[26,27] It is therefore attractive to speculate that VWF is an underestimated player in these settings. We hypothesize that a thrombolytic agent that generates plasmin in a VWF-dependent manner would also have clinical benefits in these indications.

Acknowledgments

C.M. gratefully acknowledges the Landsteiner Foundation for Blood Transfusion Research (#LSBR 1520), the Netherlands Organization for Scientific Research (NWO, 2019/TTW/00695158), and the Circulatory Health Programme of the UMC Utrecht for the Utrecht-Leuven collaboration grant. S.d.M. gratefully acknowledges the TTW section of the Netherlands Organization for Scientific Research (NWO, 2019/TTW/00704802) and T.R. grants A11/SFB877, B08/SFB841, and P06/KFO306 of the German Research Foundation (DFG). The authors would like to thank Albert Huisman and Ms. Thea Hol-Muskee for assisting in VWF-FVIII complex determinations. The authors are grateful to Ms. Wariya Sanrattana for designing the visual abstract.

Authorship

Contribution: S.d.M., C.C.C., R.T.U., P.J.L., M.S., C.H., T.R., K. Vercruysse, K. Vanhoorelbeke, C.T., and C.M. conceived and/or designed the study; S.d.M., C.C.C., A.D.B., M.W., M.v.M., N.D., S.S., N.D.v.K., and H.E.O. performed in vitro experiments; C.T. performed the in vivo TTP model and LDH activity determination; and S.d.M., C.T., and C.M. wrote the manuscript.

Conflict-of-interest disclosure: C.M. has been a speaker for Shire/Takeda on topics unrelated to this work. C.M., M.v.M., K. Vercruysse, and S.d.M. are founders of TargED BV, a biotech spinout company of University Medical Center Utrecht (to develop Microlyse). C.M. and S.d.M. participate in revenue sharing as inventors through the commercialization arm of the University Medical Center Utrecht. K. Vercruysse is a consultant to Shire/Takeda and Sanofi. The results discussed in this manuscript form part of the patent application Targeted Thrombolysis for Treatment of Microvascular Thrombosis (WO2019185723 A1). The remaining authors declare no competing financial interests.

ORCID profiles: S.d.M., 0000-0003-1179-374X; C.C.C., 0000-0001-9614-7135; A.D.B., 0000-0002-0653-5538; S.S., 0000-0002-3229-7238; N.D.v.K., 0000-0001-7162-9277; H.E.O., 0000-0002-2344-6027; M.S., 0000-0003-1553-9765; N.D., 0000-0003-4302-8233; R.T.U., 0000-0002-1601-9393; P.J.L., 0000-0002-7937-3429; C.H., 0000-0002-7114-4023; T.R., 0000-0003-4594-5975; K. Vanhoorelbeke, 0000-0003-2288-8277; C.T., 0000-0002-6380-6349; C.M., 0000-0003-4593-0976.

Correspondence: Coen Maas, University Medical Center Utrecht, Heidelberglaan 100, 3584 CX, Utrecht, The Netherlands; e-mail. cmaas4@umcutrecht.nl.

Footnotes

Submitted 19 March 2021; accepted 24 October 2021; prepublished online on *Blood* First Edition 12 November 2021. DOI 10.1182/blood.2021011776.

The online version of this article contains a data supplement.

There is a *Blood* Commentary on this article in this issue.

The publication costs of this article were defrayed in part by page charge payment. Therefore, and solely to indicate this fact, this article is hereby marked "advertisement" in accordance with 18 USC section 1734.

REFERENCES

1. George JN, Nester CM. Syndromes of thrombotic microangiopathy. *N Engl J Med.* 2014;371(19):1847-1848.
2. Sadler JE. Pathophysiology of thrombotic thrombocytopenic purpura. *Blood.* 2017; 130(10):1181-1188.
3. Peyvandi F, Scully M, Kremer Hovinga JA, et al; TITAN Investigators. Caplacizumab for acquired thrombotic thrombocytopenic purpura. *N Engl J Med.* 2016;374(6): 511-522.
4. Scully M, Cataland SR, Peyvandi F, et al; HERCULES Investigators. Caplacizumab treatment for acquired thrombotic thrombocytopenic purpura. *N Engl J Med.* 2019;380(4):335-346.
5. Tersteeg C, de Maat S, De Meyer SF, et al. Plasmin cleavage of von Willebrand factor as an emergency bypass for ADAMTS13 deficiency in thrombotic microangiopathy. *Circulation.* 2014;129(12):1320-1331.
6. Tersteeg C, Joly BS, Gils A, et al. Amplified endogenous plasmin activity resolves acute thrombotic thrombocytopenic purpura in mice. *J Thromb Haemost.* 2017;15(12): 2432-2442.
7. Wang X, Palasubramaniam J, Gkanatsas Y, et al. Towards effective and safe thrombolysis and thromboprophylaxis: preclinical testing of a novel antibody-targeted recombinant plasminogen activator directed against activated platelets. *Circ Res.* 2014;114(7):1083-1093.
8. Fuentes RE, Zaitsev S, Ahn HS, et al. A chimeric platelet-targeted urokinase prodrug selectively blocks new thrombus formation. *J Clin Invest.* 2016;126(2):483-494.
9. Tsai HM. Pathophysiology of thrombotic thrombocytopenic purpura. *Int J Hematol.* 2010;91(1):1-19.
10. Tsai HM. Physiologic cleavage of von Willebrand factor by a plasma protease is dependent on its conformation and requires calcium ion. *Blood.* 1996;87(10):4235-4244.
11. Brophy TM, Ward SE, McGimsey TR, et al. Plasmin cleaves von Willebrand factor at K1491-R1492 in the A1-A2 linker region in a shear- and glycan-dependent manner in vitro. *Arterioscler Thromb Vasc Biol.* 2017; 37(5):845-855.
12. Frenken LGJ, van der Linden RHJ, Hermans PWJJ, et al. Isolation of antigen specific llama VHH antibody fragments and their high level secretion by Saccharomyces cerevisiae. *J Biotechnol.* 2000;78(1):11-21.
13. van Driel PBAA, Boonstra MC, Slooter MD, et al. EGFR targeted nanobody-photosensitizer conjugates for photodynamic therapy in a pre-clinical model of head and neck cancer. *J Control Release.* 2016;229:93-105.
14. Liu JN, Tang W, Sun ZY, et al. A site-directed mutagenesis of pro-urokinase which

substantially reduces its intrinsic activity. *Biochemistry*. 1996;35(45):14070-14076.

15. Petersen LC. Kinetics of reciprocal pro-urokinase/plasminogen activation–stimulation by a template formed by the urokinase receptor bound to poly(D-lysine). *Eur J Biochem*. 1997;245(2):316-323.

16. Przeradzka MA, Meems H, van der Zwaan C, et al. The D′ domain of von Willebrand factor requires the presence of the D3 domain for optimal factor VIII binding. *Biochem J*. 2018;475(17):2819-2830.

17. Lee HT, Park UB, Jeong TJ, et al. High-resolution structure of the vWF A1 domain in complex with caplacizumab, the first nanobody-based medicine for treating acquired TTP. *Biochem Biophys Res Commun*. 2021;567:49-55.

18. Ts'ao C, Green D, Rossi EC. Some factors affecting fibrinogen precipitation by ristocetin: ultrastructure of precipitates. *Blood*. 1975;45(5):621-629.

19. Zheng XL, Vesely SK, Cataland SR, et al. ISTH guidelines for treatment of thrombotic thrombocytopenic purpura. *J Thromb Haemost*. 2020;18(10):2496-2502.

20. Watanabe R, Wada H, Miura Y, et al. Plasma levels of total plasminogen activator inhibitor-I (PAI-I) and tPA/PAI-1 complex in patients with disseminated intravascular coagulation and thrombotic thrombocytopenic purpura. *Clin Appl Thromb Hemost*. 2001;7(3):229-233.

21. Sargentini-Maier ML, De Decker P, Tersteeg C, Canvin J, Callewaert F, De Winter H. Clinical pharmacology of caplacizumab for the treatment of patients with acquired thrombotic thrombocytopenic purpura. *Expert Rev Clin Pharmacol*. 2019;12(6):537-545.

22. Tersteeg C, Schiviz A, De Meyer SF, et al. Potential for recombinant ADAMTS13 as an effective therapy for acquired thrombotic thrombocytopenic purpura. *Arterioscler Thromb Vasc Biol*. 2015;35(11):2336-2342.

23. Zhao T, Houng A, Reed GL. Termination of bleeding by a specific, anticatalytic antibody against plasmin. *J Thromb Haemost*. 2019;17(9):1461-1469.

24. Callewaert F, Roodt J, Ulrichts H, et al. Evaluation of efficacy and safety of the anti-VWF Nanobody ALX-0681 in a preclinical baboon model of acquired thrombotic thrombocytopenic purpura. *Blood*. 2012;120(17):3603-3610.

25. Schiviz A, Wuersch K, Piskernik C, et al. A new mouse model mimicking thrombotic thrombocytopenic purpura: correction of symptoms by recombinant human ADAMTS13. *Blood*. 2012;119(25):6128-6135.

26. Denorme F, Langhauser F, Desender L, et al. ADAMTS13-mediated thrombolysis of t-PA-resistant occlusions in ischemic stroke in mice. *Blood*. 2016;127(19):2337-2345.

27. De Meyer SF, Savchenko AS, Haas MS, et al. Protective anti-inflammatory effect of ADAMTS13 on myocardial ischemia/reperfusion injury in mice. *Blood*. 2012;120(26):5217-5223.